Ultrawideband Cavity-Backed Resistively Loaded Planar Dipole Array for Ground Penetrating Radar

Alan J. Fenn, Peter T. Hurst, Joe Pacheco, Matthew Cornick, Leonard I. Parad
Lincoln Laboratory, Massachusetts Institute of Technology, Lexington, MA 02420-9185, USA
ajf@ll.mit.edu

[1]**Abstract**— *An ultrawideband (UWB) cavity-backed resistively loaded planar dipole array antenna has been developed for the 100 to 400 MHz frequency range for ground penetrating radar applications. The antenna has been designed with a 3m aperture to perform surveys of a wide swath of ground from a moving vehicle. The performance of the UWB array is quantified by moment method simulations of the electromagnetic field penetration into lossy soil. Integration of the UWB array onto a vehicle is discussed.*

1. INTRODUCTION

Ground penetrating radar (GPR) antenna systems have been explored for a number of applications such as in noninvasive subsurface pipe detection, road and bridge inspection, geology, archaeology, and other applications as summarized by Peters [1] and Yarovoy [2] and other researchers [3-13]. It is desirable for some applications to provide ground penetrating radar (GPR) imaging capability at 0 to 1 meter (or more) depth for surveying large portions of terrain from an on-the-move vehicle with a large aperture array antenna system. In this paper, a custom 10 ft (3 m) wide antenna aperture with 24 radiating/receiving dipole antenna elements arranged in a periodic linear array covering the 100 to 400 MHz (VHF/UHF) band is explored. An artist concept of the GPR array aperture is depicted in Figure 1, where a cavity-backed antenna array is connected to a bracket that can be attached to the front or rear of the vehicle. The ground penetrating array antenna described here consists of resistively loaded printed-circuit patch dipole elements contained within a U-shaped electrically conducting cavity. Electromagnetic simulations were used in designing a field deployable dipole array antenna, which has been fabricated and installed on a ground vehicle for field testing. Section 2 describes the GPR array design approach, Section 3 describes the detailed array design and Section 4 describes the fabrication of a prototype dipole array. Electromagnetic simulations using the method of moments for the GPR array over lossy soil are presented in Section 5. Section 6 has a summary.

[1] This work is sponsored by the Department of the Army under Air Force Contract #FA8721-05-C-0002. Opinions, interpretations, conclusions and recommendations are those of the authors and are not necessarily endorsed by the United States Government.

2. ARRAY DESIGN APPROACH

This section describes the design approach for the example large-aperture ground penetrating radar ultrawideband array antenna. The prototype antenna is desired to have an aperture length of approximately 10 ft (3m) (cross-track direction), containing 24 identical antenna elements arranged periodically in a linear array with center-to-center element spacing 5.0 inches (12.7 cm), with polarization aligned in the along-track direction. The array is shown conceptually in Figure 2, in which the array elements are depicted as segmented metallic patches and can be dipole (or monopole) type antenna elements. Dipoles are appropriate to fit within the close array element spacing, and the elements are assumed to be planar to allow fabrication with printed circuit board techniques. The array is designed to operate in the 100 to 400 MHz band which allows electromagnetic penetration into soil.

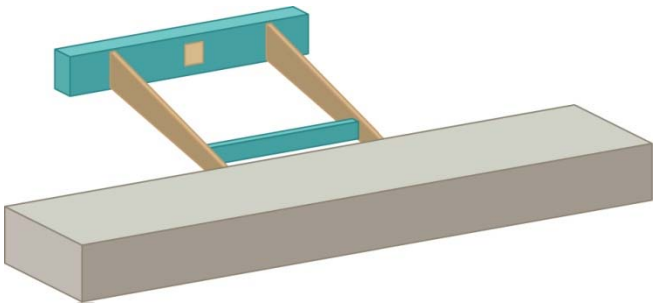

Figure 1. Conceptual view of an antenna aperture for ground penetrating radar application in which the antenna is supported by a bracket that can be mounted to the front or rear end of a ground vehicle.

Figure 2. Conceptual view of a planar dipole array in which the dipole elements would be composed of segments that are connected by resistors to reduce ringing effects. One or two passively terminated elements would surround the array to reduce edge effects.

In the along-track direction, the maximum allowed array dimension is assumed to be in the range of 2 to 3 feet (0.6m to 0.91m). The lowest point of the GPR antenna is assumed to be approximately 9 inches (22.86 cm) from the ground. The power coupled from any transmit element into any adjacent receive element must not obscure the radar target return. To reduce array element time-domain ringing, resistive loading along the length of the elements is commonly used in ground penetrating radar antennas and other antenna applications [12-16] and is the approach used here. In Figure 2, the antenna elements are shown as segments that would be interconnected by resistors (not shown). It is understood that resistive loading will lower the efficiency of the array, which will degrade the signal-to-noise ratio (SNR) and impact the detection of scatterers in the soil. To avoid array edge effects, it is necessary to provide one or two resistively loaded elements surrounding the active array. These resistively loaded surrounding elements (also referred to in the literature as dummy elements) are used to avoid an abrupt change in the element performance near the edge of the array. In Figure 2, the free-space array shown would radiate energy upward toward the sky and down toward the ground. To restrict the energy downward into the ground, it is desirable to surround the array with a metal cavity acting as a ground plane. In Figure 3 for a dipole array, the metal wall structure surrounding the array has a number of important electromagnetic characteristics including reduction of external interference (noise), reduction of vehicle scattering effects, and increasing the antenna gain in the direction of the ground.

Mechanically, the metal cavity surrounding the GPR planar dipole array has a number of useful features. The metal cavity provides a rugged support member that can be attached to a vehicle. Furthermore, the metal cavity can support the array antenna elements, feed cables, beamforming network, and protective radome.

By dividing the dipole elements into electrically conducting segments with gaps between the segments, the dipoles can be resistively loaded along their lengths, and they can also be loaded between the base of the feed region to improve the return loss and reduce ringing. The dipole array requires balanced antenna feeds to ensure that each dipole is driven symmetrically. For the prototype dipole array an ultrawideband 50-ohm transformer balun was used, which covers the desired bandwidth. The transformer balun converts an unbalanced 50-ohm coaxial line feed into a wideband 180-degree phase shift between the two balanced outputs connected to the dipole terminals. The next section provides the detailed design, and fabrication of the dipole array.

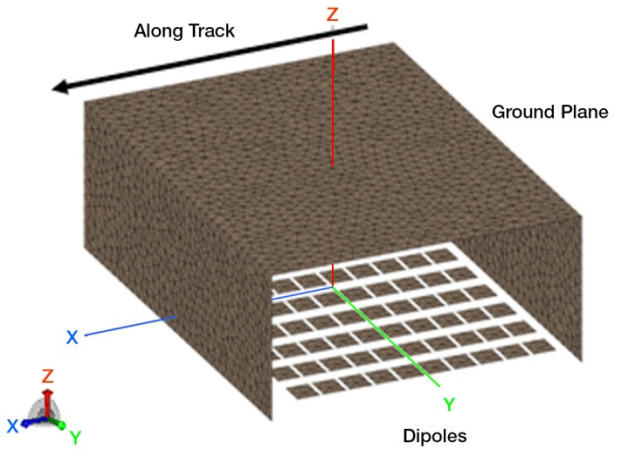

Figure 3. Cavity-backed planar dipole array for ground penetrating radar.

3. DETAILED ARRAY DESIGN

Based on method of moments electromagnetic simulations with FEKO (www.feko.info) and prototype measurements, the design of the dipole array elements is given in Figure 4. The overall length of the resistively-loaded dipole elements is 20 inches (50.8 cm). Each of the dipoles is composed of 10 metallic segments. A 0.5-inch (1.27 cm) gap is used between each of the dipole segments with the exception of the feed region which uses a 0.05-inch (1.27 mm) gap. The dipole segments are connected by pairs of resistors R1, R2, R3, R4, and R5 which have values 133, 124, 165, 255, and 536 ohms, respectively. The resistors with values Ri are connected to the dipole segments in parallel, so the total resistance at the *i*th gap is Ri/2.

Excluding the central gap, the value of the *i*th total gap resistance is determined according to the following equation (Wu and King [11]), $R_{it}=R_0/(1-x_i/(L/2))$, where R_o is taken as 50 ohms, x_i is the location of the ith resistor, and L is the length of the dipole. For example, at the dipole segment gap closest to the feed gap, the gap is located at x_2= 1.87 inches (4.75 cm) from the midpoint of the dipole. It follows from the above equation that R_{2t}=61.5 ohms and R2 = 123 ohms. The actual R2 value used was 124 ohms according to available commercial components. The values for resistors R2, R3, R4, R5 are calculated similarly. Using the above values for R2, R3, R4 and R5, the 133 ohm resistor (R1) at the center feed gap was used to make the real part of the input impedance of the loaded dipole element (simulated by the method of moments) as close to 50 ohms as possible over the 100 to 400 MHz band.

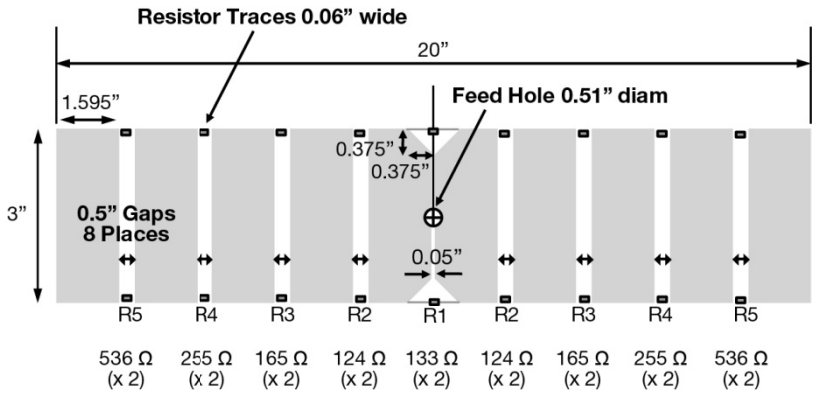

Figure 4. Design of resistively loaded planar dipole array element for the ground penetrating radar application

To illustrate the effectiveness of resistive loading in reducing signal ringing, consider the following resistively loaded (using the above resistive values) and unloaded strip dipole 2-element arrays depicted in Figure 5. The length and width of the resistively loaded and unloaded strip dipoles are 20 inches (50.8 cm) and 3 inches (7.62 cm), respectively and the center-to-center element spacing is 5.0 inches (12.7 cm). Simulated S-parameter (S21) data were computed in the frequency domain and transformed to the time domain using an inverse Fast Fourier Transform (IFFT). A comparison of the simulated time domain voltage response to a Gaussian monocycle pulse as input to resistively loaded and unloaded dipole array elements is shown in Figure 6. Clearly, the resistive loading provides significant damping of ringing compared to the unloaded strip dipole case.

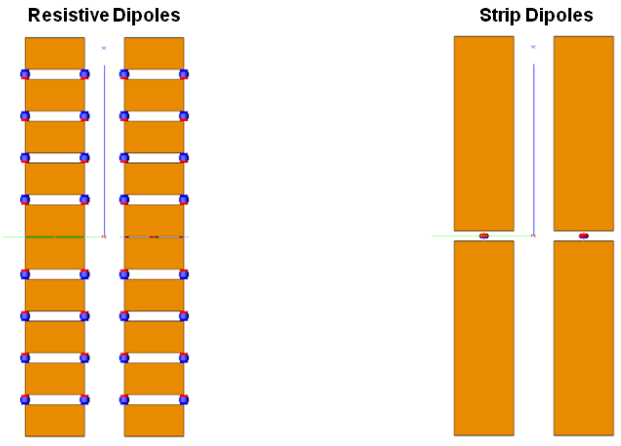

Figure 5. Depiction of resistively loaded and unloaded planar dipole array elements.

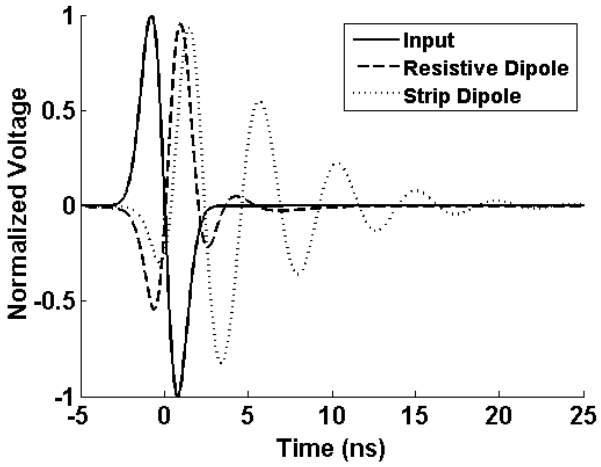

Figure 6. Simulated time domain voltage response to a Gaussian monocycle pulse as input to resistively loaded and unloaded planar dipole array elements

The dimensions of the metal waveguide cavity (120 inches long, 24 inches wide, and 12 inches high) (3.05m long, 0.61m wide, and 0.3m high) were chosen such that the full array bandwidth could be covered without generating higher order modes. In this design, the planar dipole array elements are located 10 inches (25.4 cm) from the backwall of the metallic waveguide and 2.0 inches (5.08 cm) from the opening of the waveguide.

4. PROTOTYPE ARRAY FABRICATION

A photograph of the printed-circuit UWB dipole antenna elements is shown in Figure 7. There are three dipole elements per printed circuit board in this design, thus, in the 24-element array eight printed circuit boards are used. In this photograph, chip resistors have been soldered in place at each of the gaps. A number of prototype printed-circuit dipole arrays were fabricated and one such prototype is depicted in Figures 8 and 9. The metallic waveguide was formed using 0.5-inch aluminum honeycomb material. To maintain a flat surface, the array elements are mounted on 1.5-inch (3.81 cm) thick non-conducting Nomex honeycomb material that is secured to the side walls of the waveguide. The dipoles were fed with 50-ohm coaxial cables using transformer baluns that were connected to the dipole terminals. The coaxial cable / transformer balun assembly was contained within fiberglass tubing and the balun end of the tubing was secured to the nomex honeycomb structure. In the photographs shown in Figures 8 and 9, note that the metal end caps enclosing the waveguide have not yet been installed. The array was installed on a vehicle for outdoor ground penetrating radar field testing, as depicted in Figures 10 and 11. The results of ground penetrating radar field testing are highly dependent on both the field conditions and signal processing techniques and are beyond the scope of this paper; however, electromagnetic simulations of the fields in lossy soil for this ultrawideband dipole array are described in the next section.

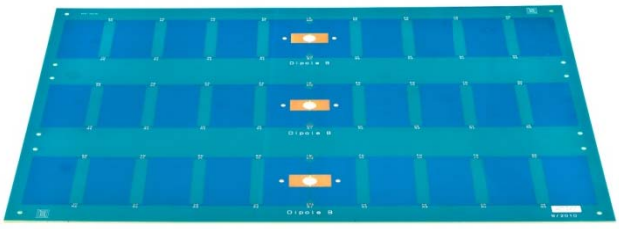

Figure 7. Photograph showing three resistively-loaded printed circuit board UWB planar dipole array elements for a prototype 24-element dipole array.

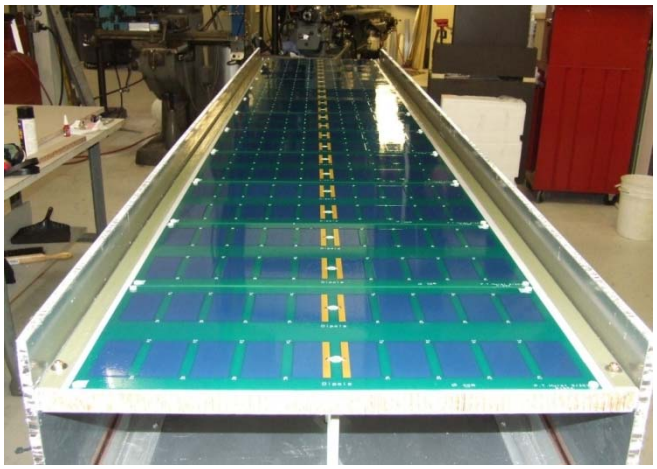

Figure 8. Photograph of a prototype 24-element ground penetrating radar UWB cavity-backed resistively-loaded planar dipole array during fabrication.

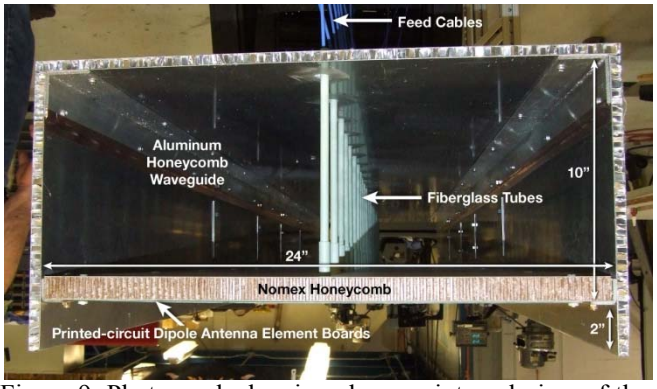

Figure 9. Photograph showing close up internal view of the 24-element GPR UWB cavity-backed planar dipole array.

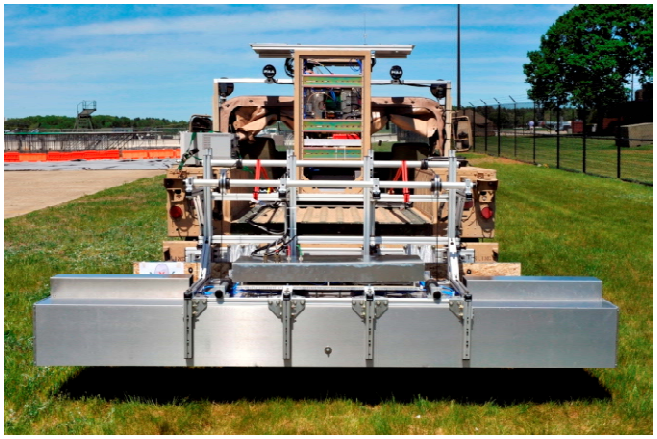

Figure 10. Photograph showing an along-track view of a prototype ground penetrating radar UWB cavity-backed planar dipole array on a vehicle for field testing.

Figure 11. Photograph showing a cross-track view of a prototype ground penetrating radar UWB cavity-backed planar dipole array on a vehicle for field testing.

5. SIMULATED RESULTS

To include the effects of array mutual coupling, the 24-element resistively loaded dipole array was analyzed with the method of moments using FEKO software. Each of the dipoles and the metallic waveguide cavity were modeled in a fine grid using electric surface-patch basis and testing functions. The total number of moment method basis functions for these simulations was 16,704. The array is assumed to be 9.0 inches (22.86 cm) above the simulated soil, which was simulated as an infinite lossy dielectric half space using the Green's function for a planar substrate. The dielectric properties of soil vary widely depending on soil type, salt content, and moisture content, and for purposes of analysis in this paper, the soil is assumed to have a dielectric constant of 6.0 and an electrical conductivity equal to 0.01 S/m. For example, at 250 MHz with these dielectric parameters the corresponding attenuation constant is computed to be 0.77 nepers/m which results in a plane-wave attenuation of 6.7 dB/m. Furthermore, the intrinsic impedance of the soil is computed as 152.5 + j 11.3 ohms, and the phase constant is 10.3 radians/m.

In the GPR array simulations, a central element is excited with a 1 watt generator and the surrounding dipole elements have their feeds terminated in 50-ohm resistive loads. The x-axis is aligned with the dipole elements and the y-axis is along the axis of the 24-element linear array. The negative z axis points down toward the simulated soil, with z = 0 being the location of the planar dipole array elements. The near-zone electric field was computed over a 3-dimensional grid of points with 31 points in x and y dimensions and 11 points in z, with 0.25m (9.84-inch) spacing between points. Figure 12 shows the electromagnetic model of the dipole array with metallic waveguide above the infinite half space. The simulated reflection coefficient amplitude versus frequency of one of the center elements (element 12) is shown in Figure 13. The reflection coefficient is better than −20 dB across the 100 to 400 MHz band. This low reflection coefficient is attributed to the use of the resistive loads connecting the dipole segments. Thus, ringing is expected to be low with this design compared to unloaded elements as demonstrated previously in Figure 6.

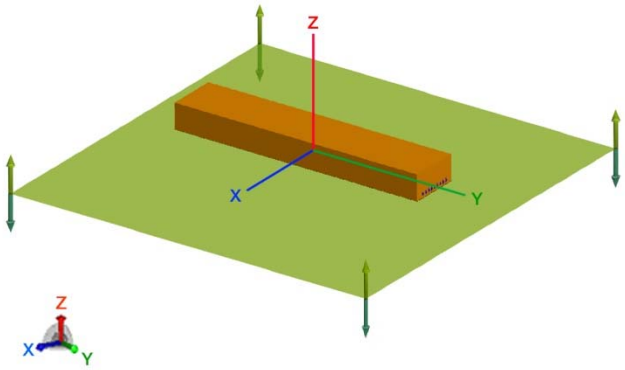

Figure 12. Electromagnetic simulation model of the GPR planar dipole array with metallic waveguide above an infinite half space representing soil.

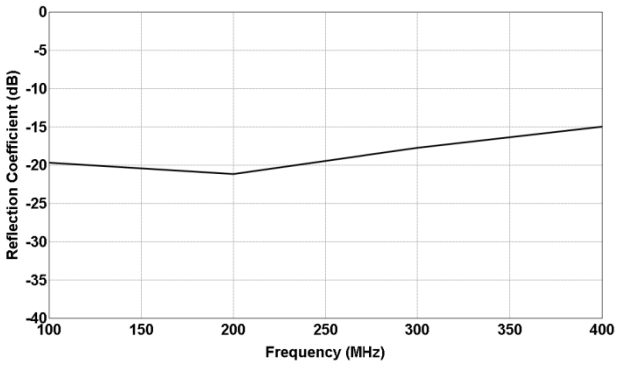

Figure 13. Simulated reflection coefficient for central dipole element number 12 in the cavity-backed resistively loaded 24-element planar dipole array over lossy soil (dielectric constant = 6, electrical conductivity = 0.01 S/m).

Assume now 1 watt transmitting power at the central antenna array element (number 12) and consider the electric field radiated into the simulated soil. The co-polarized (x-component) near-zone electric-field amplitude in dBV/m versus x position (with y = 0) at a depth of 1 meter in the soil (for 100, 200, 300, and 400 MHz) is shown in Figure 14, which is an E-plane near-field cut. The co-polarized (x-component) near-zone electric-field amplitude in dBV per meter versus y position (with x = 0) at a depth of 1 meter in the soil (for frequencies 100, 200, 300, and 400 MHz) is

shown in Figure 15, which is an H-plane near-field cut. The H-plane cut is observed to have a broader radiation pattern as would be expected. In both Figures 14 and 15, it is observed that at this fixed 1 meter depth in soil that the E-field amplitude increases with increasing frequency, due to increased gain of the dipole radiating element as it approaches an electrical length of 0.67 wavelengths at 400 MHz. At 100 MHz, the 20-inch dipoles are electrically short (only 0.17 wavelengths) and low gain would be expected. Next, in Figure 16 the E-field amplitude versus z position (at x = y = 0) is shown and the attenuation observed is a function of both the loss in the dielectric and the 1/r attenuation from the radiating dipole. Finally, in Figure 17 the E-field amplitude at various z positions (x = y = 0) below the array is shown as a function of frequency. Again, the E-field amplitude is observed to increase with increasing frequency, and decrease with increasing depth into the simulated soil below the array.

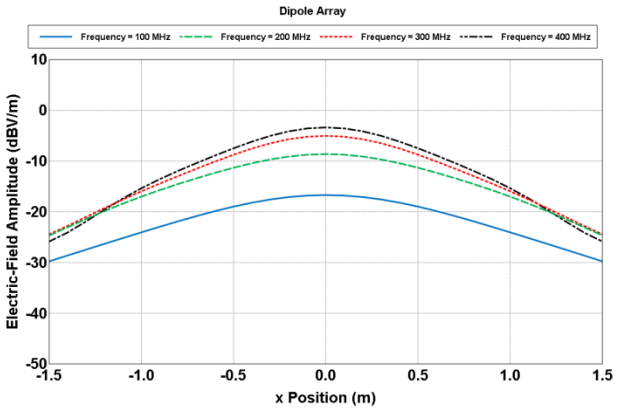

Figure 14. Simulated near-zone E-field versus x position (y = 0, E-plane cut) at 1 meter depth in lossy soil (dielectric constant = 6, electrical conductivity = 0.01 S/m) for the resistively loaded UWB dipole array.

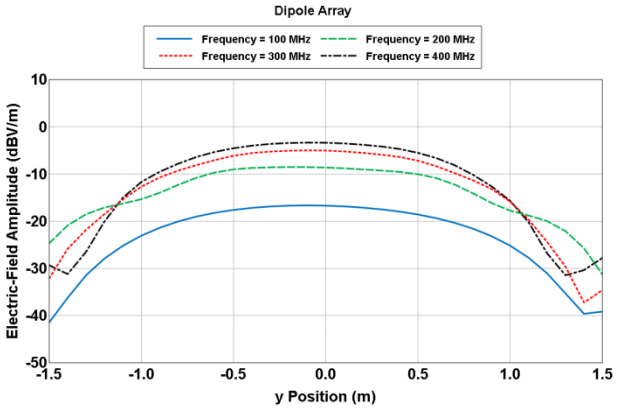

Figure 15. Simulated near-zone E-field versus y position (x = 0, H-plane cut) at 1 meter depth in lossy soil (dielectric constant = 6, electrical conductivity = 0.01 S/m) for the resistively loaded UWB 24-element dipole array.

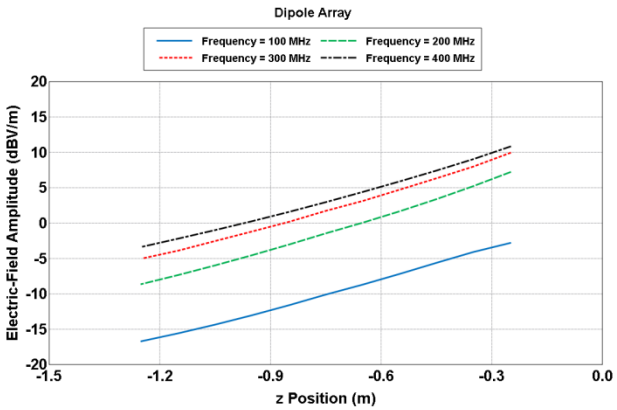

Figure 16. Simulated near-zone E-field versus z position (x = 0, y = 0) in lossy soil (dielectric constant = 6, electrical conductivity = 0.01 S/m) for the resistively loaded UWB 24-element dipole array. The position z = 0 is the location of the dipole array elements.

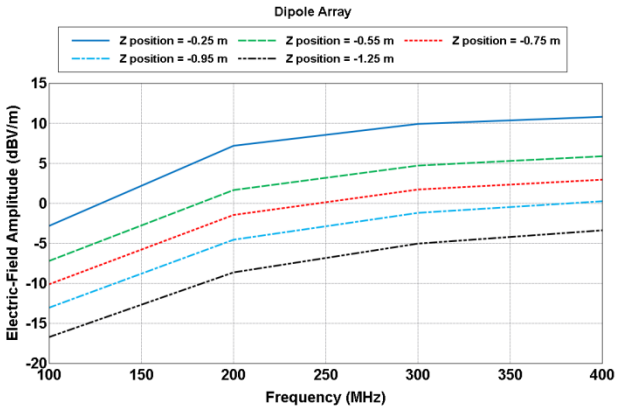

Figure 17. Simulated near-zone E-field versus frequency for various z distances (x = 0, y = 0) in lossy soil (dielectric constant = 6, electrical conductivity = 0.01 S/m) for the resistively loaded UWB 24-element dipole array.

Although not addressed here, an improved ultrawideband dipole array incorporating resistive cards (R-cards) and ferrite tiles has also been designed, built, and tested. This design improves the similarity between the array element beam patterns by mitigating cavity effects, array end effects, and element-to-element mutual coupling. The R-card design incorporates resistive film sheet between each array element, and ferrite absorbing tile coating the interior of the left and right cavity end-caps. The R-cards have been found to increase the isolation between the array elements. The addition of R-cards and ferrite tiles does not significantly impact other design criteria such as gain or bandwidth. The R-card array will be detailed in a future publication.

6. SUMMARY

An ultrawideband dipole array antenna has been developed for a ground penetrating radar application on a ground vehicle. The dipole array consists of resistively loaded printed-circuit dipole elements contained within a U-shaped electrically conducting cavity with closed conducting end caps. The resistive loading is used to reduce ringing effects. The array has 24 antenna elements and the overall length of the array is 10 feet, which could be used to perform a ground penetrating radar survey of subsurface features. The dipole array has been designed to cover the 100 to 400 MHz frequency band for transmit and receive capability. Electromagnetic simulations were used in designing a prototype array antenna, which has been fabricated and installed on a ground vehicle for field testing. The electromagnetic simulations indicate that good performance should be achieved in practice with this type of ground penetrating radar antenna array.

ACKNOWLEDGMENT

The authors would like to express their gratitude to Beijia Zhang for technical discussions throughout this project. Technical discussions with Chi-Chih Chen of The Ohio State University, ElectroScience Laboratory, are sincerely appreciated. Edwin F. LeFave, Brice K. MacLaren, Trina R. Vian, Matthew Pineau, and Thomas A. Matte provided mechanical design support and support in machining portions of the prototype antenna array. Special thanks are extended to Thomas W. Alosso, Edwin F. LeFave, and Larry Artz for fabricating the prototype array.

REFERENCES

[1] L. Peters, Jr., J.J. Daniels, and J.D. Young, Ground Penetrating Radar as a Subsurface Environmental Sensing Tool, *Proc. IEEE*, Vol. 82, December 1994, pp. 1802–1822.

[2] A. Yarovoy, editor, *Proc. 2nd Int. Workshop on Advanced Ground Penetrating Radar*, Delft, The Netherlands, May 14-16, 2003.

[3] M.I. Mirkin, C.F. Lee, T.O. Grosch, B.E. Hedges, S. Ayasli, K. Kappra, K. Sturgess, Results on ground penetration SAR phenomenology from June 1993 Yuma experiment, *IEEE 1995 Int. Radar Conference*, 1995, pp. 164-170.

[4] G.F. Stickley, D.A. Noon, M. Chernlakov, I.D. Longstaff, Preliminary field results of an ultra-wideband (10-620 MHz) stepped-frequency ground penetrating radar, *IEEE International Geoscience and Remote Sensing Symposium, IGARSS '97*, Vol. 3, 1997, pp. 1282-1284.

[5] G. Serbin and D. Or, Ground-penetrating radar measurement of soil water content dynamics using a suspended horn antenna, *IEEE Trans. Geoscience and Remote Sensing*, Vol. 42, No. 8, 2004, pp. 1695-1705.

[6] Ultrawideband Gated Step Frequency Ground-Penetrating Radar, M.J. Oyan, S. Hamran, L. Hanssen, T. Berger, D. Plettemeier, *IEEE Trans. Geoscience and Remote Sensing*, Vol. 50, No. 1, 2012, pp. 212-220.

[7] C.-C. Chen, S. Nag,W. Burnside, J. Halman, K. Shubert, and L. Peters, Jr., A standoff, focused-beam land mine radar, *IEEE Trans. Geoscience and Remote Sensing*, vol. 38, no. 1, Jan. 2000, pp. 507-514.

[8] D. Daniels, *Ground-Penetrating Radar*, 2nd ed., London, U.K., IEE, 2007.

[9] L.B. Convers, *Ground-Penetrating Radar for Archaeology,* 2nd ed*.,* AltaMira Press, 2005.

[10] H.M. Jol, editor, *Ground Penetrating Radar Theory and Applications*, Elsevier Science, Ltd., 2009.

[11] T.T. Wu and R.W.P. King, Cylindrical antenna with nonreflecting resistive loading, *IEEE Trans. Antennas and Propagat.*, Vol. AP-13, May 1965, pp. 369-373.

[12] R.E. Clapp, A resistively loaded, printed circuit, electrically short dipole element for wideband array applications, *IEEE Antennas and Propagation Society Int. Symp. Digest*, vol. 1, 1993, pp. 478-481.

[13] D. Uduwawala et al., A Deep Parametric Study of Resistor-Loaded Bow-Tie Antennas for Ground-Penetrating Radar Applications Using FDTD, *IEEE Trans. Geoscience and Remote Sensing*, Vol. 42, No. 4, April 2004, pp. 732-742.

[14] M. Kanda, A Relatively Short Cylindrical Broadband Antenna with Tapered Resistive Loading for Picosecond Pulse Measurements, *IEEE Trans. Antennas Propagat.,* Vol. AP-26, May 1978, pp. 439-447.

[15] T.P. Montoya and G.S. Smith, "Land Mine Detection Using a Ground Penetrating Radar Based on Resistively Loaded Vee Dipoles," *IEEE Trans. Antennas Propagat.*, Vol. 47, December 1999, pp. 1795-1806.